Inorganic Chemistry

Article

pubs.acs.org/IC

Composite System of Ag Nanoparticles and Metal–Organic Frameworks for the Capture and Conversion of Carbon Dioxide under Mild Conditions

Ning-Ning Zhu,[†,∥] Xiao-Huan Liu,[†,§,∥] Tao Li,[†] Jian-Gong Ma,[*,†] Peng Cheng,[†,‡] and Guang-Ming Yang[†]

[†]Department of Chemistry and Key Laboratory of Advanced Energy Material Chemistry, Nankai University, Tianjin 300071, China

[‡]Collaborative Innovation Center of Chemical Science and Engineering (Tianjin), Tianjin 300071, China

[§]College of Materials Science and Engineering, Hebei University of Engineering, Handan, Hebei 056038, China

Supporting Information

ABSTRACT: The materials Ag@MIL-100(Fe) and Ag@UIO-66(Zr) are obtained for the capture and transformation of CO_2 into alkynyl carboxylic acids, which are environmental friendly, facile to synthesize, and exhibit excellent efficiency and reusability. The influence on the catalytic activity of such Ag@MOF systems by metal–organic frameworks' (MOFs) surface area, thermal, and chemical stability, especially the acid–base characteristics of the pores, are compared and discussed systematically.

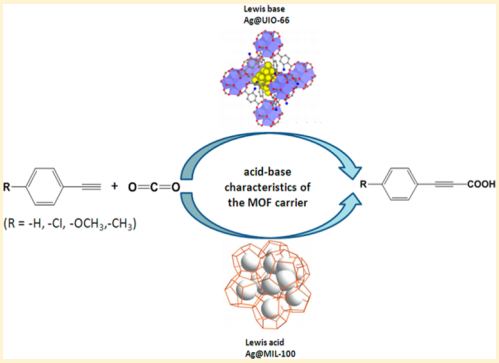

INTRODUCTION

CO_2 emission has become an urgent issue in recent decades because it is the main greenhouse gas leading to a series environmental problems.[1] Nevertheless, CO_2 is a cheap, safe, abundant, and reproducible carbon resource as well. Transforming CO_2 into valuable products is thus absolutely necessary.[2] Recently, researchers have paid attention to C–C bond-formation reactions with CO_2 as a C1 building block.[3] One of the best ways is carboxylating terminal alkynes with CO_2, which is a clean and green route to produce alkynyl carboxylic acids[4] for further application as vital intermediates in pharmacy and organic synthesis in cycloaddition, hydroarylation, and dicarboxylative cross-coupling reactions.[5,6] Many organometallic complexes with conscientiously designed ligands,[7] such as Ag(I) or Cu(I) salts system and poly-NHC supported Ag nanoparticles (NPs) material,[8,9] have been applied to catalyze this reaction. However, there are many shortcomings including high ligand sensitivity to water and air, difficulties in separation and reusability, as well as high pressure or temperature. In order to solve these problems and make the whole process more effective, researchers are currently focusing on supporting Ag NPs with carbon, silica, zeolites, or metal–organic frameworks (MOFs).[10]

Recently, MOFs have attracted great attention because of their high porosity, good gas adsorption ability, thermal stability and structural diversity.[11] On the basis of these properties, MOFs have been used in many transformation of organic reactions as heterogeneous catalysts, especially as a carrier material for the immobilization of metal NPs.[12]

In 2015, we reported the carboxylation of terminal alkynes with CO_2 carried out by a Ag@MIL-101(Cr) material, which exhibited excellent catalytic performance.[2a] Subsequently, toward the actual application as a green catalyst, further improvements of Ag@MIL-101(Cr) are still demanded: (i) Cr(III) is poisonous and one of the most concerned pollutes for water and food; (ii) in the mature process of synthesis of MIL-101(Cr), hydrofluoric acid is used, which is harmful to health conditions.[13] Besides, in comparison of MIL-101(Cr) the synthesis and postprocessing of MIL-100(Fe) is easier. In this article, we demonstrate the modification of our Ag@MIL-101(Cr) system, through using MIL-100(Fe) and UIO-66(Zr) instead of MIL-101(Cr). The materials Ag@MIL-100(Fe) and Ag@UIO-66(Zr) are highly effective for the transformation of CO_2 into alkynyl carboxylic acids, as well as more environmentally friendly, easier to synthesize, and nontoxic in comparison of Ag@MIL-101(Cr). The influence on the catalytic activity of such Ag@MOF systems by MOFs' surface area, stability, especially the acid–base characteristics of the pores, are compared and discussed systematically.[14]

Received: December 4, 2016

DOI: 10.1021/acs.inorgchem.6b02855
Inorg. Chem. XXXX, XXX, XXX–XXX

EXPERIMENTAL SECTION

Catalyst Preparation. MIL-100(Fe) was prepared through the method described in the literature.[15c] The loading of MIL-100(Fe) with Ag NPs was achieved via a simple liquid impregnation method.[2a] First, the required amount (1 g) of MIL-100(Fe) was immersed into acetonitrile solution of silver nitrate under constant stirring for 12 h at room temperature, then it was centrifuged and dried at 100 °C under vacuum to obtain Ag^+@MIL-100(Fe). The Ag^+@MIL-100(Fe) was further reduced by ethanol solution of sodium borohydride for 3 h in Ar atmosphere. The catalyst Ag@MIL-100(Fe) was gained by centrifuge and thoroughly washed by ethanol. The sample was finally dried at 100 °C under vacuum and then kept under Ar for further use. Using this procedure, samples containing 20, 30, and 50 wt % $AgNO_3$ were prepared. These will be noted as **1a**, **1b**, and **1c**.

UIO-66(Zr) was prepared through the method described in the literature.[16] The loading of UIO-66(Zr) with Ag NPs was achieved via a simple liquid impregnation method.[2a] First, the required amount (1 g) of UIO-66(Zr) was immersed into acetonitrile solution of silver nitrate under constant stirring for 12 h at room temperature, then it was centrifuged and dried at 100 °C under vacuum to obtain Ag^+@UIO-66(Zr). The Ag^+@UIO-66(Zr) was further reduced by ethanol solution of sodium borohydride for 3 h in Ar atmosphere. The catalyst Ag@UIO-66(Zr) was gained by centrifuge and thoroughly washed by ethanol. The sample was finally dried at 100 °C under vacuum and then kept under Ar for further use. Using this procedure, samples containing 5, 10, 20, and 30 wt % $AgNO_3$ were prepared. These will be noted as **2a**, **2b**, **2c**, and **2d**.

Catalyst Activity. A Schlenk tube containing a stirring bar was charged with Ag@UIO-66/Ag@MIL-100(Fe) (70 mg) and Cs_2CO_3 (1.5 mmol) inside of glovebox. Then 1-ethynylbenzene (1.0 mmol) and DMF (5 mL) were added by syringe. Once added, the Schlenk tube was placed at atmospheric pressure of CO_2 (1 atm) and stirred for 15 h at 50 °C. The mixture was centrifuged, then the liquid was hydrolyzed and extracted with CH_2Cl_2. The aqueous layer was acidized by HCl and extracted with ethyl acetate. The combined organic layers were dried over anhydrous Na_2SO_4 and evaporated.

Catalyst Characterization. NMR spectra were recorded on a Varian Inc. Mercury Vx-300 type (δ_H, 300 MHz) spectrometer. Chemical shifts were reported in ppm from tetramethylsilane with the solvent resonance as the internal standard. Data were reported in the following order: chemical shift in ppm (multiplicity was indicated by s (singlet), d (doublet), t (triplet), q (quartet), m (multiplet)). X-ray photoelectron spectroscopic (XPS) analyses were carried out on a Kratos Analytical Ltd. Axis Ultra DLD X-ray photoelectron spectrometer. The Ag content of each sample was analyzed by means of an inductively coupled plasma (ICP) spectrometer (Thermo Jarrell-Ash Corp., U.S.A.). Transmission electron microscopy (TEM) experiments were conducted on a FEI Tecnai G2 F20 electron microscope (200 kV). Powder X-ray diffraction (PXRD) data were collected by using a D/Max-2500 X-ray diffractometer with Cu Kα radiation. The EDS was measured using a JEOL JSM-7500F scanning electron microscope (SEM). The Brunauer–Emmett–Teller (BET) surface areas were screened by nitrogen adsorption and desorption at 77 K using a Quantachrome Automated Surface Area. Isotherm of carbon dioxide was measured at 298 K using a Quantachrome Autosorb-1 volumetric adsorption analyzer.

RESULTS AND DISCUSSION

Characterization of Ag@MIL-100(Fe). To avoid the pollution of Cr(III) ions and hydrofluoric acid used in Ag@MIL-101(Cr), we introduced MIL-100(Fe) as the MOF support instead of MIL-101(Cr). As given in Figure 1, the obtained Ag@MIL-100(Fe) catalysts were labeled as **1a**, **1b**, and **1c** with the Ag loading of 0.013, 0.022, and 0.035 mmol, respectively, as confirmed by ICP analyses. A close agreement between experimental PXRD patterns of catalysts **1a**–**1c** and the literature[15] has proven that the catalysts were successfully synthesized. There was no remarkable change of the pattern

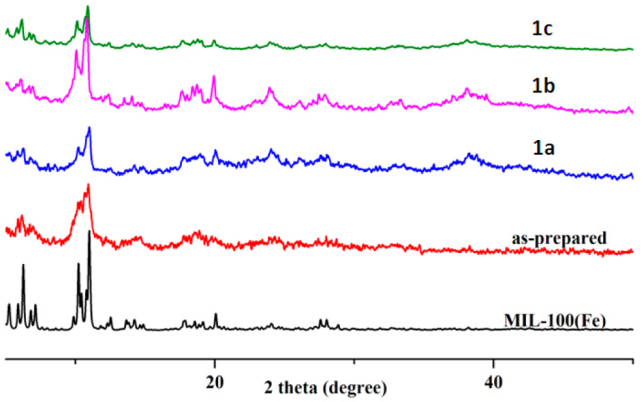

Figure 1. PXRD patterns of MIL-100(Fe), **1a**, **1b**, and **1c**.

after depositing Ag NPs, which demonstrated that the three-dimensional crystalline framework of the supporter was retained after the loading and reduction process. Some of the pores might be occupied during the preparation due to the changes that occurred in the width and relative intensity of PXRD patterns. The PXRD pattern did not exhibit the characteristic peak of Ag(111) at 2θ = 38.1° and Ag(200) at 2θ = 44.3°, probably attributed to the low Ag loading and small diameter of Ag NPs.[17,18]

Thermal degradations of the solid materials were investigated to confirm the ultimate temperature in the catalytic reaction and the thermal stability after Ag loading. As shown in Figure 2,

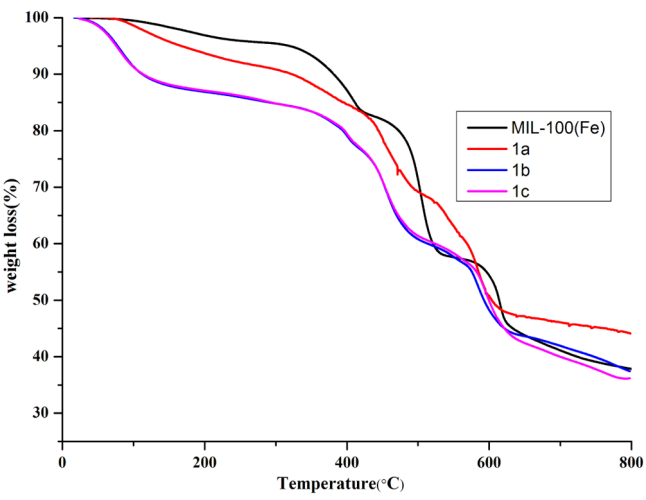

Figure 2. TGA curves for MIL-100(Fe) and **1a**, **1b**, and **1c**.

the thermogravimetric analysis (TGA) curves of MIL-100(Fe) were comparable to that in the literature.[15] **1a**, **1b**, and **1c** showed similar thermal stability, illustrating that the MIL-100(Fe) still maintained a favorable stability for all the Ag-loaded samples. When the temperature was less than 300 °C, the structure of the catalysts remained stable.

The N_2 adsorption–desorption measurement (Figure S1 in the Supporting Information) has been implemented to investigate the surface area and porous nature of MIL-100(Fe) and Ag@MIL-100(Fe) catalysts (Figure S2 and Table S1). Appreciable decreases in the amount of N_2 sorption in comparison with MIL-100 occurred for all the catalyst samples. The decreases of surface areas should be attributed to that the pores of MIL-100(Fe) might be occupied and/or

DOI: 10.1021/acs.inorgchem.6b02855
Inorg. Chem. XXXX, XXX, XXX–XXX

blocked by the Ag NPs.[19] The trend of the curves is as similar as the previous report.[15] CO_2 adsorption−desorption isotherms of activated MIL-100(Fe) and Ag@MIL-100(Fe) were examined at room temperature and atmospheric pressure (Figure 3). The adsorptive capacity of CO_2 attained 40.31, 37.14, 41.08 mg/g for **1a**, **1b**, and **1c**, respectively, providing the possibility for the subsequent reaction.

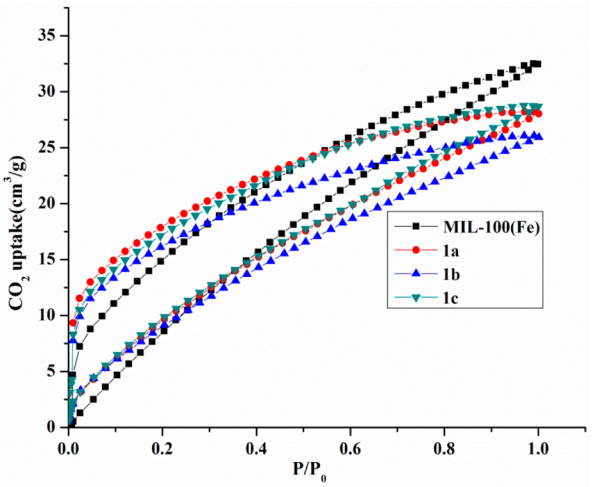

Figure 3. CO_2 adsorption−desorption of MIL-100(Fe) and Ag@MIL-100(Fe) samples with different Ag loadings at 298 K.

Successful deposition of Ag NPs at the MIL-100(Fe) is confirmed by SEM images and energydispersive spectroscopy (EDS) spectra. As shown in SEM images (Figures 4, S3, and S4), the as-prepared **1a**−**1c** were on the micrometer scale, among which **1b** exhibited the best distribution of Ag NPs, while a slight aggregation was also observed for the sample of **1c** due to its high Ag loading. The morphology of MIL-100(Fe) immobilizing Ag NPs in **1a**, **1b**, and **1c** were further characterized by TEM. The TEM images (Figures 5, S5, and S6) showed that Ag components in **1b** (1.5 ± 0.5 nm) were adequately dispersed and were controlled in smaller sizes than that in **1a** (2.2 ± 0.2 nm) and **1c** (2.0 ± 0.3 nm), all in agreement with mesoporous pores in MIL-100(Fe),[15c] suggesting that Ag NPs mainly dispersed in the cavities of the MIL-100(Fe).[20]

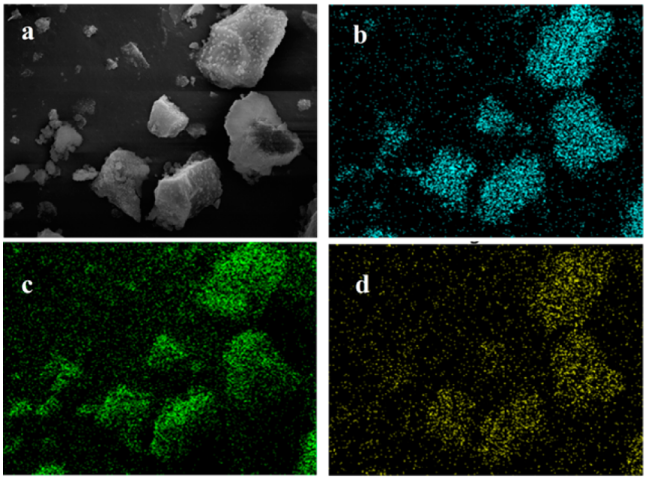

Figure 4. EDS images for the sample **1b**. (a) SEM image, (b) Fe, (c) O, and (d) Ag.

In order to investigate the state of Ag NPs in MIL-100(Fe), XPS study was executed on $AgNO_3$@MIL-100(Fe) and Ag@MIL-100(Fe) catalysts (Figure 6). As shown in Figure 6, the Ag 3d peaks of Ag@MIL-100(Fe) had an obvious shift compared to those of $AgNO_3$@MIL-100(Fe), and there was no Ag^+ peaks in the XPS spectra of Ag@MIL-100(Fe). The binding energies of Ag $3d_{3/2}$ and Ag $3d_{5/2}$ were at about 373.9 and 367.9 eV, respectively. The difference of the two peaks was 6.0 eV, which was in conformity with the standard Ag^0 spectra,[21] and confirmed the metallic state of Ag NPs in MIL-100(Fe).

Catalytic Activity of Ag@MIL-100(Fe). Ag@MIL-100(Fe) was used as catalyst for the immobilization of CO_2 with terminal alkynes into propiolic acids, and 1-ethynylbenzene was used as a model substrate. This reaction was carried out under the optimal conditions (1.5 equiv Cs_2CO_3, 1 atm CO_2, and 50 °C in DMF) as we explored for Ag@MIL-101(Cr).[2a]

An examination of the catalytic activities and acid−base characteristics of the MOF supporter showed high-catalytic activities for the carboxylation of terminal alkynes with CO_2 when strong acidic sites exist in MOF. MIL-100(Fe) had stronger Lewis acidity than MIL-101(Cr),[22] which preferred to adsorb the aromatic substrates[23] and activate the C≡C.[9,24] As a result, pure MIL-100(Fe) exhibited much higher catalytic activity than equal MIL-101(Cr). When the same amount (70 mg) of MIL-100(Fe) and MIL-101(Cr) were used as the only catalytic component, the yield of 3-phenylpropiolic acid catalyzed by MIL-100(Fe) was as twice as that by MIL-101(Cr), as shown in Table 1. To identify the effect of Ag NPs' concentration on the reaction, different amounts of $AgNO_3$ were examined. The amount of $AgNO_3$ was changed from 200 to 500 mg while the other values were constant. The yields of 3-phenylpropiolic were 75.7%, 94.6%, and 78.7%, and all of them are higher than the pure MIL-100(Fe) (46.2%). Catalyst **1b** afforded the highest product yield, which was comparable as Ag@MIL-101(Cr) with similar Ag loading. The catalytic activity increased in the following order: **1b** < **1c** < **1a**, and the results are consistent with the prediction of characterizations.

Subsequently, several kinds of typical alkyne reactants were explored for the carboxylation reaction with catalyst **1b**. As shown in Table 2, extremely excellent yields were acquired when the substituent groups of aromatic alkynes were either electron-donating or electron-withdrawing under these optimal conditions.

The reusability of this catalyst was then studied and the results were generalized in Figure 7. When the reaction was over, the catalyst was separated by centrifugation, washed with DMF, water, and methanol, dried at 100 °C under vacuum, and then reused for the following reactions. The catalyst **1b** was reused at least five times with barely any loss of catalytic activity, and the ICP data (0.021 mmol) as well as TEM measurement (Figure S7) of the regenerated catalyst confirmed the stability of Ag@MIL-100(Fe) catalyst during the reactions.

Characterization of Ag@UIO-66(Zr). To study the effect of the Lewis basicity on catalytic activity, Ag@UIO-66(Zr) catalysts were prepared. The obtained Ag@UIO-66(Zr) catalysts from 5, 10, 20, and 30 wt % $AgNO_3$ were labeled as **2a**, **2b**, **2c**, and **2d**, respectively, with the Ag loading of 1.20, 3.91, 7.12, and 14.85 wt %, respectively. The prepared catalysts were characterized by PXRD analysis. As can be seen, after

DOI: 10.1021/acs.inorgchem.6b02855
Inorg. Chem. XXXX, XXX, XXX−XXX

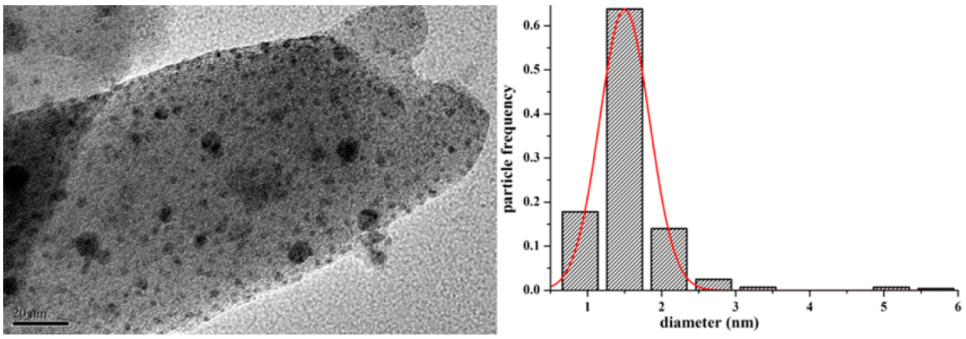

Figure 5. TEM images of sample **1b** and the size distribution of Ag NPs.

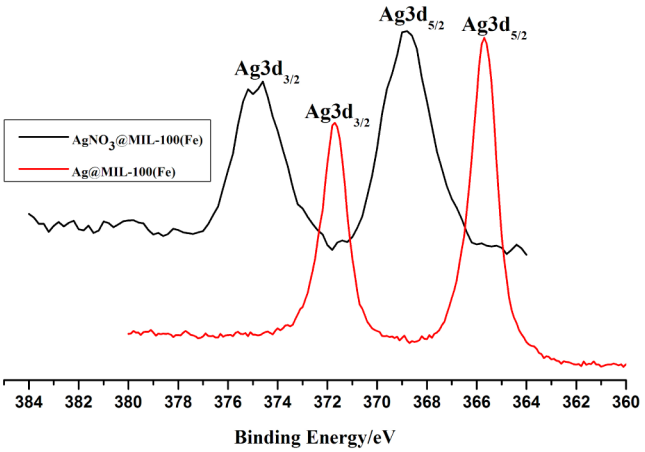

Figure 6. XPS spectra for $AgNO_3$@MIL-100(Fe) and catalyst Ag@MIL-100(Fe) showing Ag $3d_{3/2}$ and $3d_{5/2}$.

Table 1. Carboxylation Reaction from CO_2 and 1-Ethynylbenzene by Catalysts 1[a]

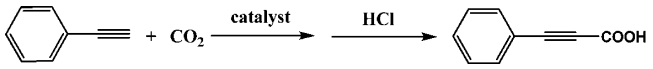

catalyst (amount, mg)	Ag loading (mmol)[b]	yield (%)[c]
MIL-100(Fe) (70)	0	46.2
MIL-101(Cr) (70)	0	21.9
Ag@MIL-101(Cr)	0.027	96.5
1a (70)	0.013	75.7
1b (70)	0.022	94.6
1c (70)	0.035	78.7

[a]Reaction conditions: catalyst (70 mg), 1-ethynylbenzene (1.0 mmol), Cs_2CO_3 (1.5 mmol), *N*,*N*-dimethylformamide (5 mL), CO_2 (1.0 atm), 50 °C, 15 h. [b]Analytical results of ICP. [c]Yield of isolated product.

loading of Ag there is almost no obvious loss of crystal form according to the PXRD pattern, which indicates that the basic lattice structure of UIO-66 was well maintained (Figure 8). The sharp peaks implied the typical crystal form of the framework. New reflection peaks consistent to the characteristic peaks of Ag(111) and Ag(200) were observed and became stronger as the increase of Ag loading, which confirmed the successful deposition of Ag NPs within the porous UIO-66(Zr). N_2 and CO_2 adsorption−desorption isotherms (Figures S8−S10 and Table S2) of Ag@UIO-66(Zr) catalysts were similar to the Ag@MIL-100(Fe) catalysts. The uptake of CO_2 reached 41.66, 44.32, 56.16, and 52.00 mg/g for **2a**, **2b**, **2c**, and **2d** respectively. Ag@UIO-66(Zr) catalysts exhibited better CO_2 absorption abilities than Ag@MIL-100(Fe) or Ag@MIL-101(Cr) due to the stronger Lewis basicity of UIO-66(Zr), which is more favorable for the capture of CO_2.[25]

Table 2. Various Propiolic Acids from Different Terminal Alkynes Catalyzed by Catalyst 1b[a]

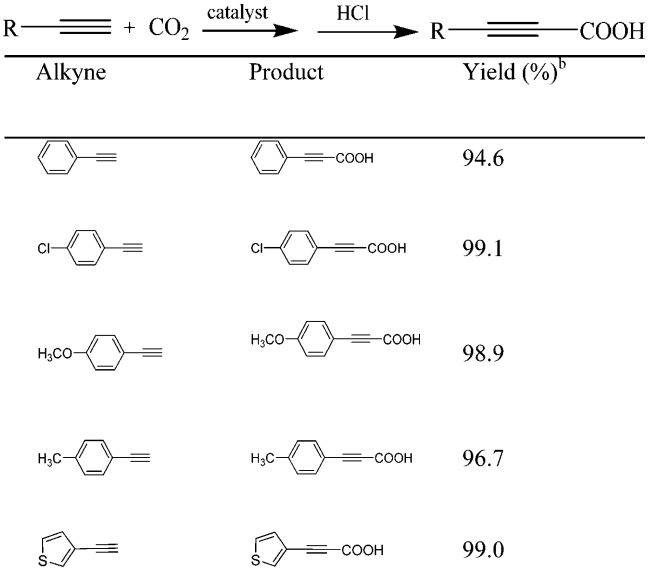

[a]Reaction conditions: catalyst **1b** (70 mg), alkynes (1.0 mmol), Cs_2CO_3 (1.5 mmol), *N*,*N*-dimethylformamide (5 mL), CO_2 (1.0 atm), 50 °C, 15 h. [b]Yield of Isolated product.

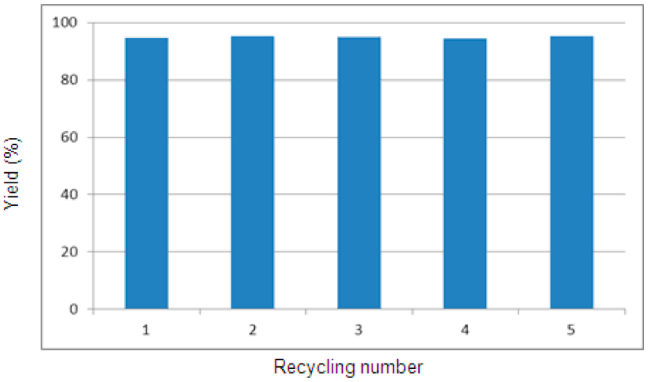

Figure 7. Recycling tests of the catalyst **1b** for the reaction of terminal alkynes with CO_2.

At first, **2a**−**2d** were used as catalysts for the model reaction and **2c** afforded the highest product yield, which was thus further characterized by SEM, TEM, and XPS. The EDS results,

DOI: 10.1021/acs.inorgchem.6b02855
Inorg. Chem. XXXX, XXX, XXX−XXX

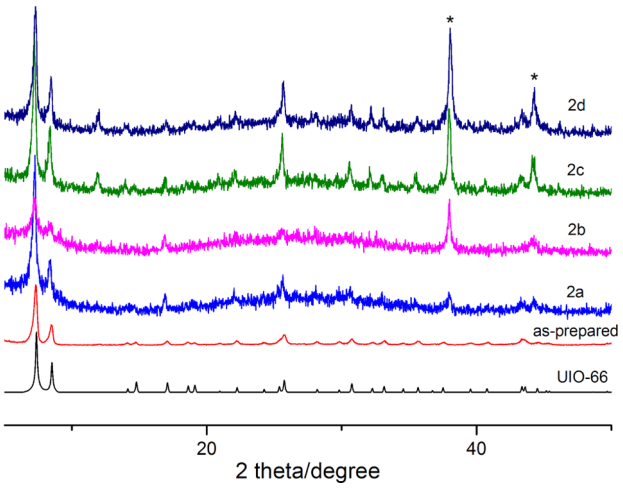

Figure 8. XRD patterns of UIO-66(Zr) and **2a**, **2b**, **2c**, and **2d**. (*) stands for the reflection peaks of crystalline Ag phases.

obtained from SEM analysis for **2c** clearly showed the existence of Ag NPs in the framework of UIO-66(Zr) (Figure S11). The TEM images showed Ag NPs with an average diameter of 1.35 nm (Figure S12). The Ag NPs were mainly dispersed in the pores of the UIO-66(Zr) and exhibited no apparent aggregation. Because UIO-66(Zr) has much stronger Lewis basicity, the Ag NPs also deposited on the external surface of it, indicating that the catalytic reaction proceeded on the surface and internal of the UIO-66(Zr) simultaneously. In the XPS of **2c**, the $3d_{3/2}$ and $3d_{5/2}$ peaks of the Ag^0 appear at 373.5 and 367.4 eV, respectively (Figure S13). No obvious peak of Ag^+ is observed, indicating that Ag is in the reduced form.

Catalytic Activity of Ag@UIO-66(Zr). Catalytic reactions for terminal alkynes and CO_2 with **2c** as well as corresponding comparison reactions were carried out with the same conditions as the Ag@MIL-100(Fe) system. A yield as high as 97.7% was obtained for 1-ethynylbenzene, and good yields were obtained as well when different substituted terminal alkynes were employed as the substrates (Table S3). **2c** could be easily regenerated and reused in the model reaction for three times without obvious loss of conversion efficiency, while after the fourth round an obvious decrease of the catalytic efficiency occurred (from 97.7% to 62.1%) and the PXRD pattern (Figure S15) showed that the frame of the catalyst collapsed. After the catalytic reactions, Ag loading of **2c** decreased to 0.035 mmol, indicating a great loss of Ag NPs, the TEM images of which (Figure S17) showed a serious aggregation of Ag NPs. Because of the narrow pore diameter of UIO-66(Zr), the reactant was difficult to come out of the pore. When the reactants accumulated to a certain amount, the framework of catalyst was easy to collapse. Besides, a part of Ag nanoparticles was deposited on the surface of the catalyst, and it was easy to fall off, leading to a poor stability and reusability.

Results and Discussion. The catalytic parameters of MOF MIL-101(Cr), MIL-100(Fe), and UIO-66(Zr) as well as composite catalysts Ag@MIL-101(Cr), Ag@MIL-100(Fe) (**1b**) and Ag@UIO-66(Zr) (**2c**) were summarized for comparison in Table 3. First, the mechanism of this Ag@MOF system should be the same:[2,9] The Ag nanoparticles coordinate to the terminal alkyne and the sp3-H bond was activated. Deprotonation of terminal alkyne by Cs_2CO_3 eventually provided a Ag acetylide along with cesium bicarbonate, and then CO_2 inserted into the C−Ag bond to

Table 3. Carboxylation Reactions of CO_2 and 1-Ethynylbenzene Catalyzed by 1 and 2[a]

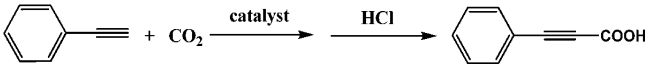

catalyst (amount, mg)	$AgNO_3$ dosage (%)[b]	Ag loading (mmol)[c]	yield (%)[d]
MIL-101(Cr) (70)	0	0	21.9
MIL-100(Fe) (70)	0	0	46.2
UIO-66(Zr) (70)	0	0	39.2
Ag@MIL-101(Cr)	30	0.027	96.5
1b (70)	30	0.022	94.6
2c (70)	20	0.046	97.7

[a]Reaction conditions: catalyst (70 mg), 1-ethynylbenzene (1.0 mmol), Cs_2CO_3 (1.5 mmol), *N*,*N*-dimethylformamide (5 mL), CO_2 (1.0 atm), 50 °C, 15 h. [b]The proportion of $AgNO_3$ with supporter. [c]Analytical results of ICP. [d]Yield of isolated product.

form the carboxylic acid products. The Lewis acidity of the framework should contributed to promote the reaction. The proposed catalytic process is shown in Figure 9.

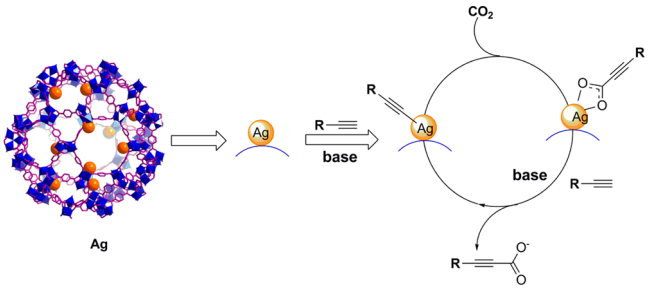

Figure 9. Proposed mechanism of the reaction between terminal alkynes with CO_2 over Ag@MOFs.

MIL-100(Fe) has stronger Lewis acidity than MIL-101(Cr),[22] which preferred to adsorb the aromatic substrates[23] and activate the C≡C.[9,24] Therefore, pure MIL-100(Fe) exhibited much higher catalytic activity than MIL-101(Cr). When the same amount (70 mg) of MIL-100(Fe) and MIL-101(Cr) were used as the only catalytic component, the yield of 3-phenylpropiolic acid catalyzed by MIL-100(Fe) was as twice as that by MIL-101(Cr). When the similar amount Ag NPs was loaded, Ag@MIL-100(Fe) exhibited excellent catalytic activity and reusability as Ag@MIL-101(Cr). However, in comparison of MIL-101(Cr), Fe(III) is nontoxic and environmentally friendly, and the synthesis of MIL-100(Fe) is easier.

As we know, UIO-66(Zr) has much stronger Lewis basicity than MIL-101(Cr), which is better for the capture and conversion of CO_2.[25] As a result, UIO-66(Zr) exhibited higher catalytic activity than MIL-101(Cr) as well. Above all, under the dual effects of Lewis acidity and Lewis basicity, the catalytic activity of pure MOF supporters shows the order of MIL-100(Fe) > UIO-66(Zr) > MIL-101(Cr). On the other hand, more basic sites in MOF could provide more coordination potential and stronger interaction for metal ions.[26,27] which facilitates the adsorption of Ag^+ by UIO-66(Zr). As shown in Table 3, although the amount of $AgNO_3$ precursor is less for UIO-66(Zr) (20%) than that for MIL-101(Cr) (30%) and MIL-100(Fe) (30%), the loading amount of Ag NPs in Ag@UIO-66(Zr) (0.046 mmol) is almost as twice as that in Ag@

DOI: 10.1021/acs.inorgchem.6b02855
Inorg. Chem. XXXX, XXX, XXX−XXX

MIL-101(Cr) (0.027 mmol) and Ag@MIL-100(Fe) (0.022 mmol), which is more economical and practical.

CONCLUSIONS

In conclusion, the Ag@MOF system exhibited excellent activity and reusability for capture and conversion of CO_2 under mild conditions. As the subsequent work following Ag@MIL-101(Cr), modification and improvement was carried on through using MIL-100(Fe) and UIO-66(Zr) instead of MIL-101(Cr) as the MOF support. In comparison with Ag@MIL-101(Cr), Ag@MIL-100(Fe) revealed similar catalytic activity, stability, and reusability but was more friendly to the environment and easier to synthesize. On the other hand, Ag@UIO-66(Zr) was more efficient and economical for the capture of CO_2 and the doping of Ag NPs but shows low reusability due to its narrow channel. On the basis of the full characterization and catalytic tests, acid−base properties of the MOF influence the catalytic activity of Ag@MOF system significantly. Stronger Lewis acidity prefers to adsorb the aromatic substrates and activate the C≡C, while stronger Lewis basicity is better for the capture of CO_2 and the loading of Ag NPs. Also, the pore size, absorptivity, and stability should be taken into account as well. On the basis of the systematically investigation, we could design suitable Ag@MOF catalysts and achieve the optimum environmental and economic benefit according to corresponding requirements toward the capture and transformation of CO_2.

ASSOCIATED CONTENT

Supporting Information

The Supporting Information is available free of charge on the ACS Publications website at DOI: 10.1021/acs.inorgchem.6b02855.

Details of experiments and characterizations (PDF)

AUTHOR INFORMATION

Corresponding Author

*E-mail: mvbasten@nankai.edu.cn.

ORCID

Jian-Gong Ma: 0000-0001-7407-5521

Peng Cheng: 0000-0003-0396-1846

Author Contributions

‖N.-N..Z. and X.-H.L. contributed to this work equally.

Notes

The authors declare no competing financial interest.

ACKNOWLEDGMENTS

This work was supported by National Key Projects for Fundamental Research and Development of China (2016YFB0600902).

REFERENCES

(1) Pervaiz, M.; Sain, M.-M. Carbon Storage Potential in Natural Fiber Composites. *Resour. Conserv. Recycl.* **2003**, *39*, 325−340.

(2) (a) Liu, X.-H.; Ma, J.-G.; Niu, Z.; Yang, G.-M.; Cheng, P. An Efficient Nanoscale Heterogeneous Catalyst for the Capture and Conversion of Carbon Dioxide at Ambient Pressure. *Angew. Chem., Int. Ed.* **2015**, *54*, 988−991. (b) He, M.-Y.; Sun, Y.-H.; Han, B.-X. Green Carbon Science: Scientific Basis for Integrating Carbon Resource Processing, Utilization, and Recycling. *Angew. Chem., Int. Ed.* **2013**, *52*, 9620−9633. (c) Aresta, M.; Dibenedetto, A.; Angelini, A. Catalysis for the Valorization of Exhaust Carbon: from CO_2 to Chemicals, Materials, and Fuels. *Chem. Rev.* **2014**, *114*, 1709−1742. (d) Gao, W.-Y.; Chen, Y.; Niu, Y.; Williams, K.; Cash, L.; Perez, P.-J.; Wojtas, L.; Cai, J.; Chen, Y.-S.; Ma, S. Crystal Engineering of An Nbo Topology Metal−organic Framework for Chemical Fixation of CO_2 under Ambient Conditions. *Angew. Chem., Int. Ed.* **2014**, *53*, 2615−2619. (e) Yu, T.; Cristiano, R.; Weiss, R.-G. From Simple, Neutral Triatomic Molecules to Complex Chemistry. *Chem. Soc. Rev.* **2010**, *39*, 1435−1447. (f) Gao, W.-Y.; Wu, H.; Leng, K.; Sun, Y.; Ma, S. Inserting CO_2 into Aryl C− H Bonds of Metal−Organic Frameworks: CO_2 Utilization for Direct Heterogeneous C−H Activation. *Angew. Chem., Int. Ed.* **2016**, *55*, 5472−5476. (g) Gao, W.-Y.; Tsai, C.-Y.; Wojtas, L.; Thiounn, T.; Lin, C.-C.; Ma, S. (2016). Interpenetrating Metal−Metalloporphyrin Framework for Selective CO_2 Uptake and Chemical Transformation of CO_2. *Inorg. Chem.* **2016**, *55*, 7291−7294.

(3) (a) Eghbali, N.; Li, C.-J. Conversion of Carbon Dioxide and Olefins into Cyclic Carbonates in Water. *Green Chem.* **2007**, *9*, 213−215. (b) Riduan, S.-N.; Zhang, Y. Recent Developments in Carbon Dioxide Utilization under Mild Conditions. *Dalton Trans.* **2010**, *39*, 3347−3357. (c) Arakawa, H.; Aresta, M.; Armor, J.-N.; Barteau, M.-A.; Beckman, E.-J.; Bell, A.-T.; Bercaw, J.-E.; Creutz, C.; Dinjus, E.; Dixon, D.-A.; Domen, K.; DuBois, D.-L.; Eckert, J.; Fujita, E.; Gibson, D.-H.; Goddard, W.-A.; Goodman, D.-W.; Keller, J.; Kubas, G.-J.; Kung, H.-H.; Lyons, J.-E.; Manzer, L.-E.; Marks, T.-J.; Morokuma, K.; Nicholas, K.-M.; Periana, R.; Que, L.; Rostup-Nielson, J.; Sachtler, W.-M.-H.; Schmidt, L.-D.; Sen, A.; Somorjai, G.-A.; Stair, P.-C.; Stults, B.-R.; Tumas, W. Catalysis Research of Relevance to Carbon Management: Progress, Challenges, and Opportunities. *Chem. Rev.* **2001**, *101*, 953−996. (d) Boogaerts, I.-I.-F.; Nolan, S.-P. Carboxylation of C−H Bonds Using *N*-Heterocyclic Carbene Gold(I) Complexes. *J. Am. Chem. Soc.* **2010**, *132*, 8858−8859. (e) Zhang, L.; Cheng, J.; Ohishi, T.; Hou, Z. Copper-Catalyzed Direct Carboxylation of C−H Bonds with Carbon Dioxide. *Angew. Chem.* **2010**, *122*, 8852−8855. (f) Correa, A.; Martin, R. Palladium-Catalyzed Direct Carboxylation of Aryl Bromides with Carbon Dioxide. *J. Am. Chem. Soc.* **2009**, *131*, 15974−15975. (g) Fujihara, T.; Xu, T.; Semba, K.; Terao, J.; Tsuji, Y. Copper-Catalyzed Silacarboxylation of Internal Alkynes by Employing Carbon Dioxide and Silylboranes. *Angew. Chem.* **2011**, *123*, 543−547.

(4) (a) Boogaerts, I.-I.-F.; Nolan, S.-P. Carboxylation of C−H Bonds Using *N*-Heterocyclic Carbene Gold(I) Complexes. *J. Am. Chem. Soc.* **2010**, *132*, 8858−8859. (b) Zhang, L.; Cheng, J.-H.; Ohishi, T.; Hou, Z.-M. Copper-Catalyzed Direct Carboxylation of C−H Bonds with Carbon Dioxide. *Angew. Chem., Int. Ed.* **2010**, *49*, 8670−8673. (c) He, H.; Perman, J.-A.; Zhu, G.; Ma, S. Metal-Organic Frameworks for CO_2 Chemical Transformations. *Small* **2016**, *12*, 6309−6324.

(5) (a) Jia, W.; Jiao, N. Cu-Catalyzed Oxidative Amidation of Propiolic Acids Under Air via Decarboxylative Coupling. *Org. Lett.* **2010**, *12*, 2000−2003. (b) Moon, J.; Jang, M.; Lee, S. Palladium-Catalyzed Decarboxylative Coupling of Alkynyl Carboxylic Acids and Aryl Halides. *J. Org. Chem.* **2009**, *74*, 1403−1406.

(6) (a) Correa, A.; Martin, R. Metal-Catalyzed Carboxylation of Organometallic Reagents with Carbon Dioxide. *Angew. Chem., Int. Ed.* **2009**, *48*, 6201−6204. (b) Bonne, D.; Dekhane, M.; Zhu, J. Modulating the Reactivity of α-Isocyanoacetates: Multicomponent Synthesis of 5-Methoxyoxazoles and Furopyrrolones. *Angew. Chem., Int. Ed.* **2007**, *46*, 2485−2488.

(7) (a) Diez-Gonzalez, S.; Nolan, S.-P. N-Heterocyclic Carbene-Copper(I) Complexes in Homogeneous Catalysis. *Synlett* **2007**, *2007*, 2158−2167. (b) Jurkauskas, V.; Sadighi, J.-P.; Buchwald, S.-L. Conjugate Reduction of α,β-Unsaturated Carbonyl Compounds Catalyzed by a Copper Carbene Complex. *Org. Lett.* **2003**, *5*, 2417−2420.

(8) (a) Zhang, X.; Zhang, W.-Z.; Ren, X.; Zhang, L.-L.; Lu, X.-B. Ligand-Free Ag(I)-Catalyzed Carboxylation of Terminal Alkynes with CO_2. *Org. Lett.* **2011**, *13*, 2402−2405. (b) Yu, D.-Y.; Zhang, Y.-G. Proc. Copper-and Copper−N-heterocyclic Carbene-catalyzed C− H Activating Carboxylation of Terminal Alkynes with CO_2 at Ambient Conditions. *Proc. Natl. Acad. Sci. U. S. A.* **2010**, *107*, 20184−20189.

(9) Yu, D.-Y.; Tan, M.-X.; Zhang, Y.-G. Carboxylation of Terminal Alkynes with Carbon Dioxide Catalyzed by Poly(N-Heterocyclic

DOI: 10.1021/acs.inorgchem.6b02855
Inorg. Chem. XXXX, XXX, XXX−XXX

Carbene)-Supported Silver Nanoparticles. *Adv. Synth. Catal.* **2012**, *354*, 969−974.
(10) (a) Jeena, S.-E.; Selvaraju, T. Facile Growth of Ag@Pt Bimetallic Nanorods on Electrochemically Reduced Graphene Oxide for an Enhanced Electrooxidation of Hydrazine. *J. Chem. Sci.* **2016**, *128*, 357−363. (b) Zhao, Z.-Y.; Vulcano Rossi, V.-A.; Baltrus, J.-P.; Ohodnicki, P.-R.; Carpenter, M.-A. Ag Nanoparticles Supported on Yttria-Stabilized Zirconia: A Synergistic System within Redox Environments. *J. Phys. Chem. C* **2016**, *120*, 5020−5032. (c) Ji, T.; Chen, L.; Mu, L.-W.; Yuan, R.-X.; Wang, H.-Y.; Knoblauch, M.; Bao, F.-S.; Zhu, J.-H. Heterogeneous Nucleation/Growth of Silver Nanoparticles onto Oxygenated Mesoporous Carbon: Alcohol Effect and Catalytic Property. *Catal. Commun.* **2016**, *77*, 65−69.
(11) (a) Kitagawa, S.; Kitaura, R.; Noro, S. Functional Porous Coordination Polymers. *Angew. Chem., Int. Ed.* **2004**, *43*, 2334−2375. (b) Kreno, L.-E.; Leong, K.; Farha, O.-K. Metal−Organic Framework Materials as Chemical Sensors. *Chem. Rev.* **2012**, *112*, 1105−1125.
(12) (a) Dhakshinamoorthy, A.; Garcia, H. Catalysis by Metal Nanoparticles Embedded on Metal−organic Frameworks. *Chem. Soc. Rev.* **2012**, *41*, 5262−5284. (b) Corma, A.; Garcıa, H.; Llabrés, F.-X.; Xamena, I. Engineering Metal Organic Frameworks for Heterogeneous Catalysis. *Chem. Rev.* **2010**, *110*, 4606−4655. (c) Li, H.; Eddaoudi, M.; O'Keeffe, M.; Yaghi, O.-M. Design and Synthesis of an Exceptionally Stable and Highly Porous Metal-organic Framework. *Nature* **1999**, *402*, 276−279.
(13) Margui, E.; Iglesias, M.; Camps, F.; Sala, L.; Hidalgo, M. Long-term Use of Biosolids as Organic Fertilizers in Agricultural Soils: Potentially Toxic Elements Occurrence and Mobility. *Environ. Sci. Pollut. Res.* **2016**, *23*, 4454−4464.
(14) Guillerm, V.; Ragon, F.; Dan-Hardi, M.; Devic, T.; Vishnuvarthan, M.; Campo, B.; Vimont, A.; Clet, G.; Yang, Q.; Maurin, G.; Ferey, G.; Vittadini, A.; Gross, S.; Serre, C. A Series of Isoreticular, Highly Stable, Porous Zirconium Oxide Based Metal−Organic Frameworks. *Angew. Chem., Int. Ed.* **2012**, *51*, 9267−9271.
(15) (a) He, J.; Wang, J.-Q.; Chen, Y.-J.; Zhang, J.-P.; Yan, Z.-Y. A Dye-sensitized Pt@UiO-66(Zr) Metal−organic Framework for Visible-light Photocatalytic Hydrogen Production. *Chem. Commun.* **2014**, *50*, 7063−7066. (b) Leus, K.; Concepcion, P.; Vandichel, M.; Van Der Voort, P. Au@ UiO-66: A Base Free Oxidation Catalyst. *RSC Adv.* **2015**, *5*, 22334−22342. (c) Seo, Y.-K.; Yoon, J.-W.; Lee, J.-S.; Lee, U.-H.; Hwang, Y.-K.; Jun, C.-H.; Horcajada, P.; Serre, C.; Chang, J.-S. Large Scale Fluorine-free Synthesis of Hierarchically Porous Iron(III) Trimesate MIL-100(Fe) with A Zeolite MTN Topology. *Microporous Mesoporous Mater.* **2012**, *157*, 137−145.
(16) Cavka, J.-H.; Jakobsen, S.; Olsbye, U.; Guillou, N.; Lamberti, C.; Bordiga, S.; Lillerud, K.-P. A New Zirconium Inorganic Building Brick Forming Metal Organic Frameworks with Exceptional Stability. *J. Am. Chem. Soc.* **2008**, *130*, 13850−13851.
(17) Jiang, H.-L.; Akita, T.; Ishida, T.; Haruta, M.; Xu, Q. Synergistic Catalysis of Au@Ag Core−Shell Nanoparticles Stabilized on Metal−Organic Framework. *J. Am. Chem. Soc.* **2011**, *133*, 1304−1306.
(18) Zahmakiran, M.; Ayvali, T.; Akbayrak, S.; Caliskan, S.; Celik, D.; Ozkar, S. Zeolite Framework Stabilized Nickel(0) Nanoparticles: Active and Long-lived Catalyst for Hydrogen Generation from the Hydrolysis of Ammonia-borane and Sodium Borohydride. *Catal. Today* **2011**, *170*, 76−84.
(19) Kardanpour, R.; Tangestaninejad, S.; Mirkhani, V.; Moghadam, M.; Mohammadpoor-Baltork, I.; Khosropour, A.-R.; Zadehahmadi, F. Highly Dispersed Palladium Nanoparticles Supported on Amino Functionalized Metal-organic Frameworks as An Efficient and Reusable Catalyst for Suzuki Cross-coupling Reaction. *J. Organomet. Chem.* **2014**, *761*, 127−133.
(20) Li, P.-Z.; Aranishi, K.; Xu, Q. ZIF-8 Immobilized Nickel Nanoparticles: Highly Effective Catalysts for Hydrogen Generation from Hydrolysis of Ammonia Borane. *Chem. Commun.* **2012**, *48*, 3173−3175.
(21) Moulder, J.-F.; Stickle, W.-F.; Sobol, P.-E. Standard Spectra for Identification and Interpretation of XPS data. Perkin-Eden: MN, 1992.
(22) (a) Vimont, A.; Goupil, J.-M.; Lavalley, J.-C.; Daturi, M.; Surble, S.; Serre, C.; Millange, F.; Ferey, G.; Audebrand, N. Investigation of Acid Sites in a Zeotypic Giant Pores Chromium(III) Carboxylate. *J. Am. Chem. Soc.* **2006**, *128*, 3218−3227. (b) Yoon, J.-W.; Seo, Y.-K.; Hwang, Y.-K.; Chang, J.-S.; Leclerc, H.; Wuttke, S.; Bazin, P.; Vimont, A.; Daturi, M.; Bloch, E.; Llewellyn, P.-L.; Serre, C.; Horcajada, P.; Grenèche, J.-M.; Rodrigues, A.-E.; Ferey, G. Controlled Reducibility of a Metal−Organic Framework with Coordinatively Unsaturated Sites for Preferential Gas Sorption. *Angew. Chem., Int. Ed.* **2010**, *49*, 5949−5952.
(23) (a) Liu, H.-L.; Li, Y.-W.; Luque, R.; Jiang, H.-F. A Tuneable Bifunctional Water-Compatible Heterogeneous Catalyst for the Selective Aqueous Hydrogenation of Phenols. *Adv. Synth. Catal.* **2011**, *353*, 3107−3113. (b) Yuan, B.-Z.; Pan, Y.-Y.; Li, Y.-W.; Yin, B.-L.; Jiang, H.-F. A Highly Active Heterogeneous Palladium Catalyst for the Suzuki−Miyaura and Ullmann Coupling Reactions of Aryl Chlorides in Aqueous Media. *Angew. Chem., Int. Ed.* **2010**, *49*, 4054−4058.
(24) Kubota, T.; Hayakawa, I.; Mabuse, H.; Mori, K.; Ushikoshi, K.; Watanabe, T.; Saito, M. Kinetic Study of Methanol Synthesis from Carbon Dioxide and Hydrogen. *Appl. Organomet. Chem.* **2001**, *15*, 121−126.
(25) Kim, J.-S.-N.; Jang, H.-G.; Seo, G.; Ahn, W.-S. CO_2 Cycloaddition of Styrene Oxide over MOF Catalysts. *Appl. Catal., A* **2013**, *453*, 175−180.
(26) Guo, Z.-Y.; Xiao, C.-X.; Maligal-Ganesh, R.-V.; Zhou, L.; Goh, T.-W.; Li, X.-L.; Tesfagaber, D.; Thiel, A.; Huang, W.-Y. Pt Nanoclusters Confined within Metal−Organic Framework Cavities for Chemoselective Cinnamaldehyde Hydrogenation. *ACS Catal.* **2014**, *4*, 1340−1348.
(27) Long, J.; Wang, S.; Ding, Z.; Zhou, Y.; Huang, L.; Wang, X. Amine-functionalized Zirconium Metal−organic Framework as Efficient Visible-light Photocatalyst for Aerobic Organic Transformations. *Chem. Commun.* **2012**, *48*, 11656−11658.

DOI: 10.1021/acs.inorgchem.6b02855
Inorg. Chem. XXXX, XXX, XXX−XXX